

DEVELOPMENT OF VORONOI MESHING METHOD CAPABLE OF REPRODUCING ARBITRARY SHAPE FOR RBSM ANALYSIS

Muhammad Shoaib KARAM*¹, Yoshihito YAMAMOTO*², Koji IKUMA*³ and Hikaru NAKAMURA*⁴

ABSTRACT

The use of new precast jointing and anchoring methods have increased and the meso-scale simulations are effective for performance evaluation and detailed fracture process. The Voronoi diagram is essential to reproduce the fracture characteristics of concrete in RBSM, however, it is difficult to express geometrical details of deformed rebars by Voronoi polyhedron. Therefore, the mesh generation method to generate arbitrary shapes by Voronoi polyhedron is proposed and validated through numerical simulation of RC prisms which efficiently reproduces the test failure mode and bond behavior in RBSM. **Keywords:** Voronoi mesh generation of arbitrary shape, meso-scale simulation analysis, coupled RBSM and solid FEM model, Goto cracks

1. INTRODUCTION

In recent years, new construction methods for improving productivity such as precast joint method, anchoring method, and so on have been developed, actively. For performance evaluation or optimization of new construction methods, not only experiments but also simulations are effective, especially meso-scale simulations. Meso-scale simulations can reproduce the crack propagation and detailed fracture behaviors around joints and anchorage and are particularly efficient.

The Rigid-Body-Spring Model (RBSM) can easily and accurately reproduce cracks, shear transfer of cracked surfaces and compression failure, etc. of concrete material and structure, compared with FEM [1-3]. There are many applications that have shown the usefulness of meso-scale simulation using RBSM [4-6].

On the other hand, previous studies have shown that the use of random polyhedron using Voronoi diagram is essential to accurately reproduce the fracture characteristics of concrete using RBSM [7-8]. However, it is difficult to express detailed shapes such as rib of deformed reinforcing bars, mechanical anchors and shear stud dowels etc. using Voronoi polyhedron, therefore high costs for mesh generation has also been a problem.

In this study, the method to generate arbitrary shapes such as geometric shapes of deformed rebars relatively easily using Voronoi polyhedron has been proposed for meso-scale simulations using RBSM. In addition, some examples of mesh generation and the mesoscale simulation of reinforced concrete are presented to show the validity and usefulness of the proposed mesh generation method.

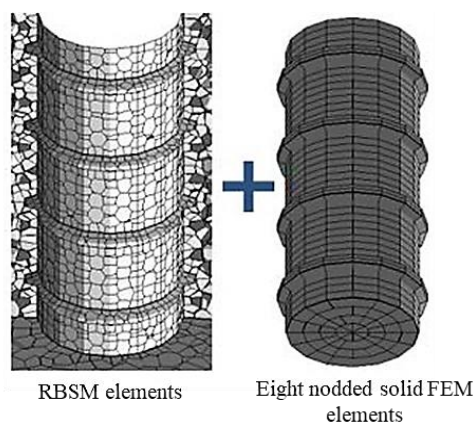


Fig. 1 Coupled RBSM and solid FEM

2. NUMERICAL MODELS

In this chapter, meso-scale simulation method for steel-concrete composite structures using RBSM is described. Although RBSM is suitable for reproducing the fracture behavior of concrete, reproducing the elasto-plastic behavior of steel is still an issue. Therefore, in this study, the method of coupled RBSM and solid FEM method which can accurately reproduce the elasto-plastic response of steel proposed by the authors [9] is applied and shown in Fig. 1.

2.1 Modeling of Concrete

Concrete is modeled using RBSM. In RBSM, concrete is modeled as a set of rigid elements, with springs placed at the interface of each element. Each rigid particle has three translational and three rotational degrees of freedom defined at the nuclei that define the particles according to the Voronoi diagram as shown in

*1 PhD Student, Dept. of Civil Engineering, Nagoya University, JCI Student Member

*2 Associate Professor, Dept. of Civil Engineering, Nagoya University, Dr.E., JCI Member

*3 Engineer, Civil & Arch. Engineering Dept., Electric Power Development Co., Master E., Non JCI Member

*4 Professor, Dept. of Civil Engineering, Nagoya University, Dr.E., JCI Member

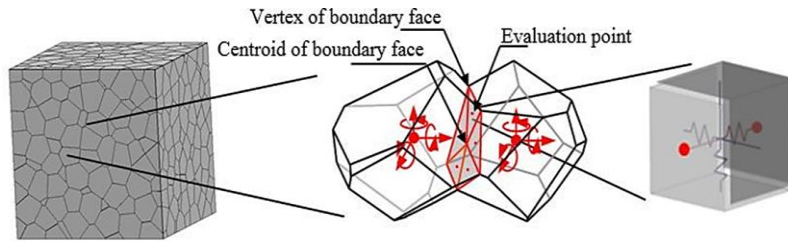


Fig. 2 3D-RBSM and Voronoi diagram (Yamamoto et al., 2008)

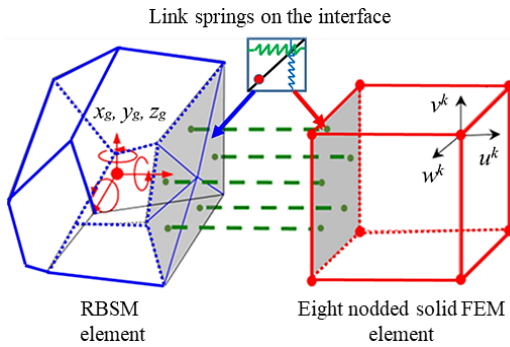


Fig. 3 Coupled RBSM-FEM interface

the Fig. 2. The boundary surface of two particles is divided into several triangles with a center of gravity and vertices of the surface. One normal and two shear springs are set at the center of each triangle. The normal spring represent compression and tension behaviors of material, and the shear spring represent shear slip behaviors. The Constitutive models and their material parameters proposed by Yamamoto et al. [1] are applied to the springs. It has been confirmed that this model can quantitatively reproduce the average stress-strain response under various stresses including the softening and localization behavior of concrete materials using element size of several mm to several tens mm.

2.2 Modeling of Steel and Concrete-Steel Interface

The steel embedded in concrete is modeled using eight-noded nonlinear FEM. A Von Mises plasticity model with strain hardening is used for the constitutive model for steel.

The interfaces between concrete and steel elements have been accomplished through link element. The link element on the interface consists of two shear springs and one normal spring as shown in Fig. 3. The constitutive model of the normal spring and the shear spring of the interface is the same as that applied to concrete [1]. However, the tensile strength of the normal spring on the interface is set half that of concrete considering the weakness of the interface [4]. The deformation of each spring of link element is obtained by the relative displacement between the surfaces of both elements.

3. VORONOI MESH GENERATION METHOD FOR ARBITRARY SHAPE

The Voronoi mesh generation method of an arbitrary target shape is discussed here. The Voronoi diagram involves the introduction of finite number of generating points defined in space and the space is

divided into number of Voronoi regions based on the nearest generating points information [10]. The feature of area dividing approach has been shown in Fig. 4. The Fig. 4 shows that Voronoi generating points are highlighted by red dots for Voronoi region, share a common boundary which is equidistant from both sides of the Voronoi generating points. The Voronoi division uses the feature that the perpendicular bisecting plane between the generating points is the area, that is, the element surface. In 3D, this region has the property of being random polyhedron geometry. The utilization of this aspect allows the development of an automatic Voronoi mesh generation method for RBSM capable of generating Voronoi meshing of an arbitrary shape.

The Voronoi mesh generation flow is described here. In the proposed meshing method, firstly the FEM mesh of the target shape is prepared using general purpose FEM software, capable of developing complex shapes such as deformed rebar with geometrical details (core diameter, rib height, shape and lug spacing, etc.) are defined, precisely. Afterwards, the information is gathered for the internal and model surface and the shared nodes between the adjacent elements of the FEM mesh as shown in Fig. 5. The Fig. 6 shows the outline of the Voronoi generating points around the FEM model surface. Initially, the internal generating points are placed randomly inside each FEM element as shown by red dots. The placement method of generating point uses the shape function of FEM. The average element size is selected in advance and the generating points are generated repeatedly inside the FEM mesh. Furthermore, external generating points are also placed outside the FEM model surface as shown by green dots in Fig. 6 symmetrical to internal generating points, in order to reproduce the target shape, then the Voronoi division is performed based on the Voronoi generating point information. The surface generated as a result of Voronoi division is referred as Voronoi surface. In this regard, the schematic flow of Voronoi mesh generation method is shown in Fig.7 and represents the Voronoi mesh generation of target shape followed by FEM mesh.

The proposed Voronoi meshing method easily reproduced the Voronoi generating points in convex part having an acute angle part as shown in Fig. 8, when inside generating point is given at random position an acute convex shape is reproduced by placing the generating point at position symmetrical to two surfaces. The same process is also performed for 90 degrees convex shape case as shown in Fig. 8. However, in convex processing of obtuse angle as shown in Fig. 9, it is observed that it is difficult to reproduce the target shape if the generating point is placed at the position as

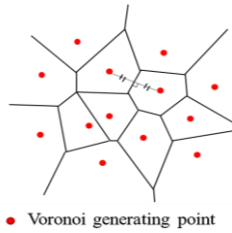


Fig. 4 Representation of Voronoi generation

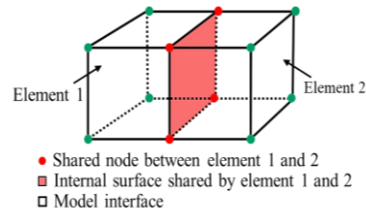


Fig. 5 Face definition of FEM mesh

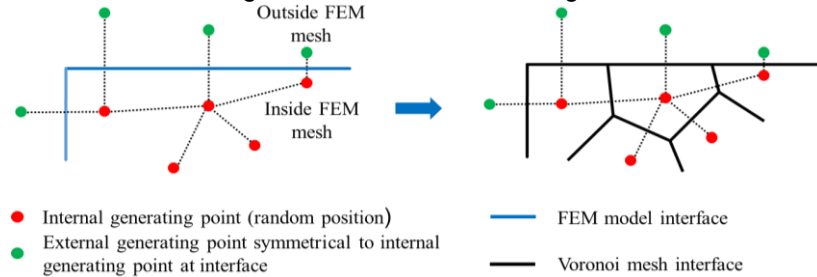


Fig. 6 Arrangement of Voronoi generating points

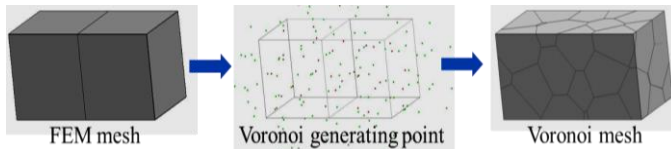


Fig. 7 Voronoi mesh generation from FEM mesh

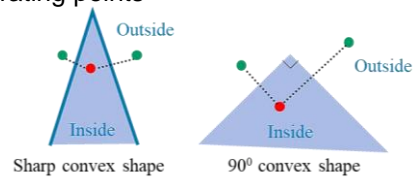


Fig. 8 Generating points for acute convex shape

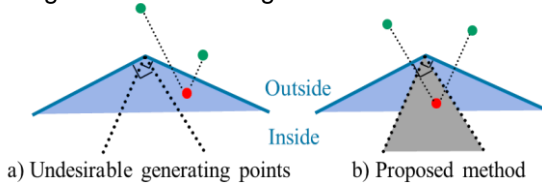


Fig. 9 Convex processing (Obtuse angle)

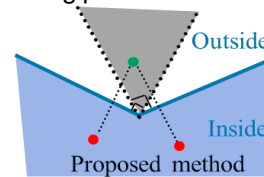


Fig. 10 Concave processing

shown in Fig. 9(a) which is undesirable. Therefore, to avoid the occurrence of situation shown in Fig. 9(a), the method has been proposed as shown in Fig. 9(b). Firstly, the angle between the convex surfaces is calculated and if it is an obtuse angle then the proposed meshing method always reproduces the condition as shown in Fig. 9(b). For this purpose, the generating point is always set inside area perpendicular to the surface and symmetrical external generating point is also set on the surface to reproduce it as shown in Fig. 9(b) and the undesirable situation never happens in proposed Voronoi meshing method. In case of the concave part as shown in the Fig. 10, the external generating point is placed in the area shown in the Fig. 10 for both acute and obtuse angles, and the internal generating point is placed symmetrically to the surface. Therefore, in the proposed Voronoi meshing method, the concave shape and the convex shape are searched beforehand and the generating points are arranged, accordingly so that the shape of the model interface can be reproduced with respect to the concave shape and the convex shape, respectively.

In addition, processing is performed for 3D unevenness such as region near to the rebar core and rebar lug as shown in Fig 11 which includes the intersection of concave and convex sides. The processing of 3D uneven shapes is carried out as when a concave side and a convex side intersect, as shown in the Fig. 12, one element represents one surface and when multiple obtuse convex parts intersect, multiple surface

is expressed as shown in the Fig. 13. In this manner, the uneven shape is searched and processed. The Fig.14 shows the Voronoi mesh generation of deformed rebar, and Perforated rib shear connector (PBL), created from FEM mesh using the proposed meshing technique. The Fig. 14 shows that firstly the FEM meshes of the deformed rebar and PBL are modeled, afterwards generating points are arranged following the desired or target shape. The Voronoi division is performed after that depending on the information of generating points. It can be observed from Fig. 14, the proposed Voronoi mesh generation method effectively reproduces the Voronoi mesh of PBL and the deformed rebar which has concave-convex sides.

4. VALIDATION OF THE PROPOSED METHOD

The validity of proposed Voronoi generation method has been performed here using the test investigations by Goto [11-12]. It is important to mention here that Voronoi mesh for RBSM is created using the FEM mesh as described in Chapter 3, excluding for the deformed rebar and then combined with a separately prepared FEM mesh that reproduces the shape of the deformed reinforcing bar. The concrete around rebar is RBSM and modelled based on the proposed meshing technique whereas steel rebar based on FEM.

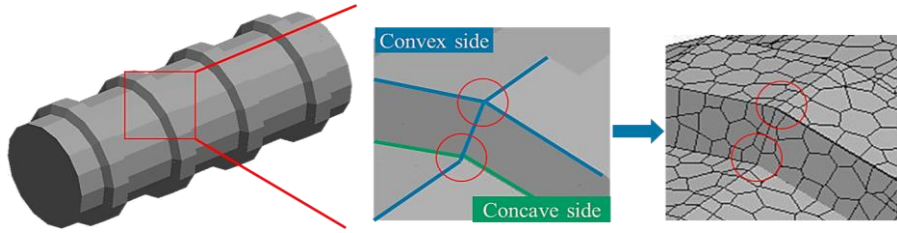


Fig. 11 Reproduction of complex shapes by 3D unevenness

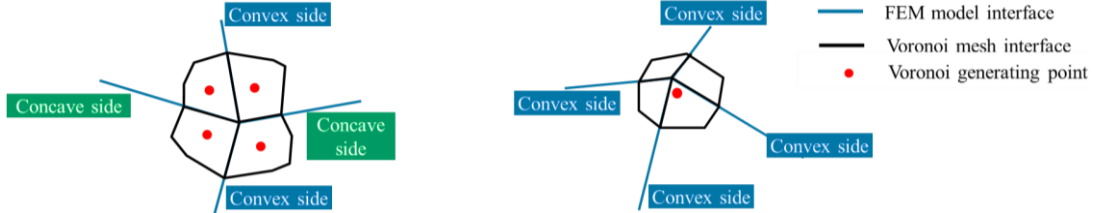


Fig. 12 Intersection of concave and convex sides

Fig. 13 Intersection of multiple convex sides

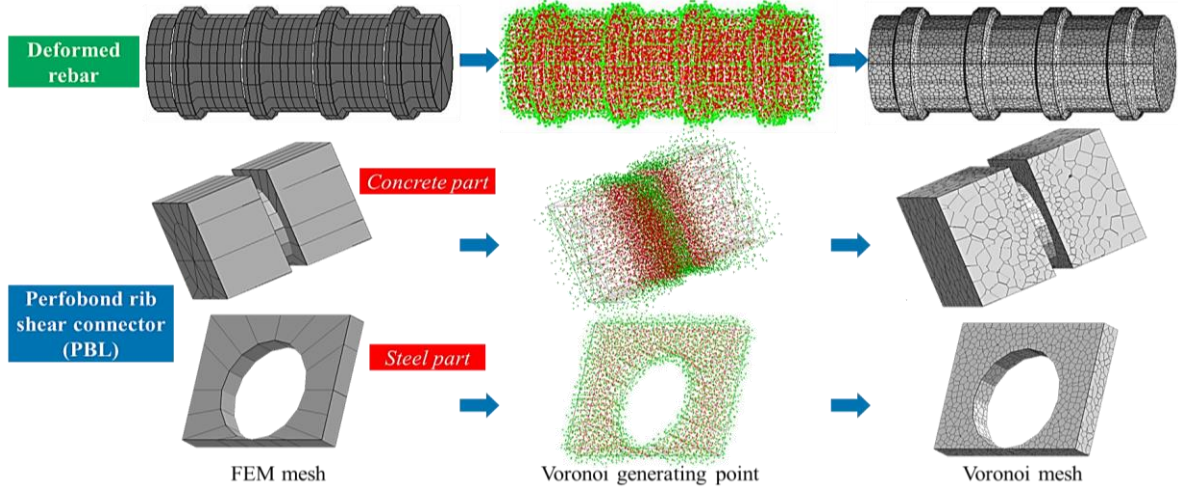


Fig. 14 Voronoi mesh of deformed rebar and Perfobond rib shear connector

4.1 Test Overview and Numerical Modeling

The meso-scale simulations using the proposed method have been carried out for the axially loaded RC prisms in tension evaluating the detailed failure mechanism [11-12]. In test, the internal crack patterns corresponding to the stress of steel were investigated around the deformed rebar using axially loaded RC prism in tension. The size of the test specimen for internal and longitudinal crack investigations were $120 \times 120 \times 1000 \text{ mm}^3$ and $120 \times 120 \times 880 \text{ mm}^3$, respectively and were embedded with rebar D32. The yield strength (f_y) of the steel used in the test was 390 MPa. The cylinder compressive strength of the concrete was around 30.0 MPa. The tensile loading was applied to exposed ends of the rebar. The internal crack formation was observed by ink injection during loading, the internal cracks were dyed and crack formation was inspected. The shallow notches were introduced in specimens before conducting the test such that first crack would occur there. The geometrical details and numerical model of test specimens are shown in Fig. 15. The numerical model includes complete modeling of concrete region without making test shallow notches as shown in Fig. 15. However, to incorporate the test shallow notches, the material parameters (tensile strength (σ_t), cohesion (c) and fracture energy (g_f)) of the constitutive models for the normal and shear springs for

concrete on the locations of the notches have been reduced by 70 % over the full cross sectional area such that primary cracks would occur there. The objective of the experiment was to reveal quantitative fracture process of axially loaded specimens. The numerical model of test specimens with D32 shown in Fig. 15, has average mesh size ranges between 2 mm to 10 mm to reduce the computational cost. Apart from previously mentioned test specimens, the numerical investigation is also extended for test specimens ($180 \times 180 \times 300 \text{ mm}^3$) with rebar D51 having lug spacing 15 mm and 30 mm as shown in Fig. 16 and average mesh ranges between 2.3 mm to 10 mm, here. The lengths of specimens in simulation analysis are selected between two experimental notches in order to reduce the mesh computational cost.

4.2 Results and Discussion

The deformed behaviors and bond strength of test specimens are discussed here. The results for cracking behaviors around rebar are simulated and are reported near to final test stress stage of rebar in numerical analysis. The internal cracks are comprised of primary and secondary cracks in test. The cracks formed firstly lateral to the rebar axis are designated as primary cracks. After the formation of primary cracks, the new cracks also propagate near to these cracks and join primary

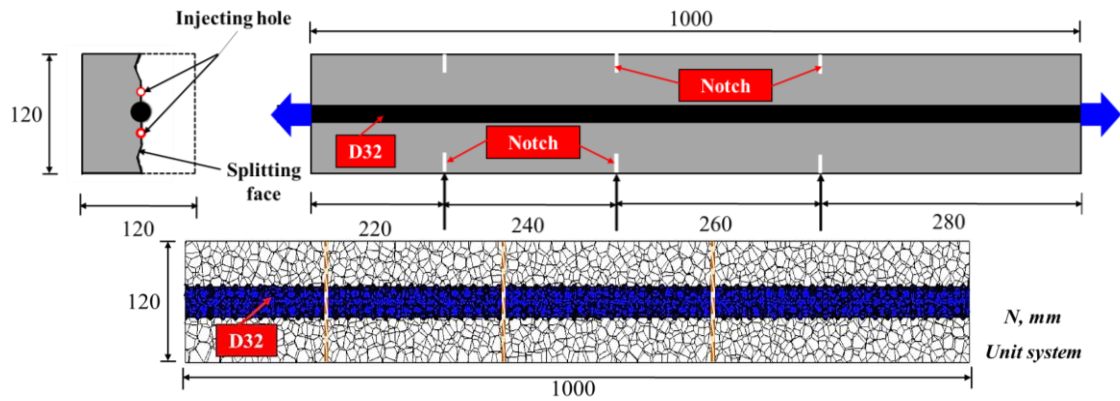


Fig. 15 Geometrical details and numerical model of test specimens

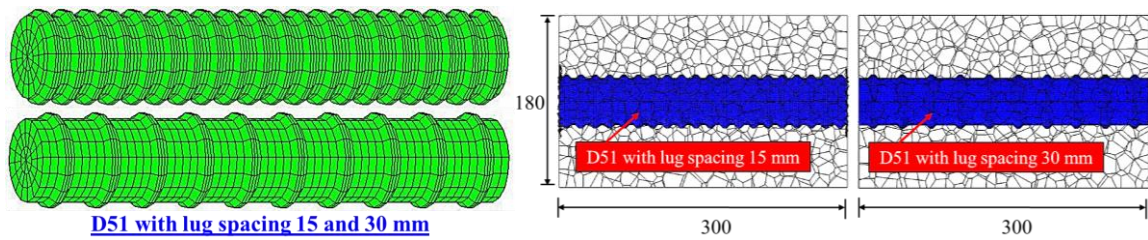
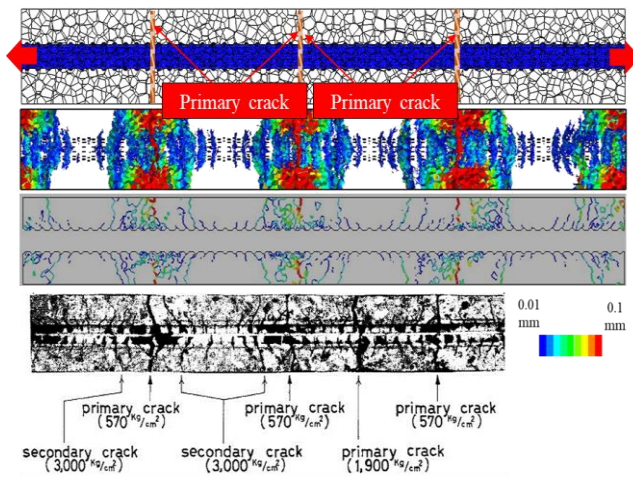
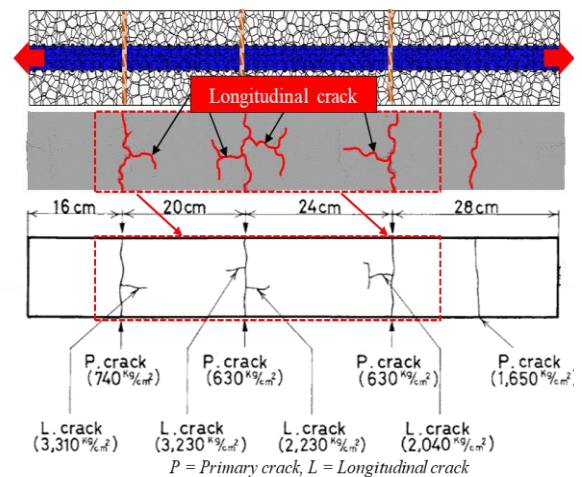


Fig. 16 Numerical model of test specimen with rebar D51



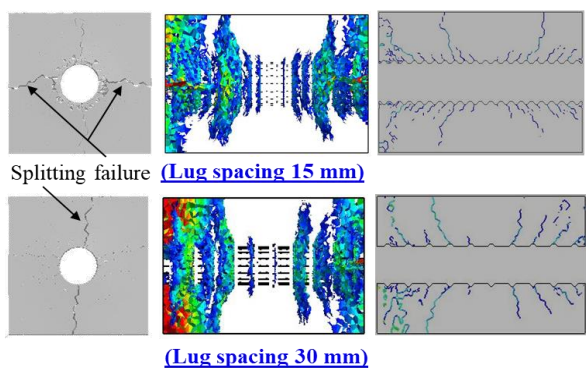
(Test result)

Fig. 17 3D and internal crack pattern



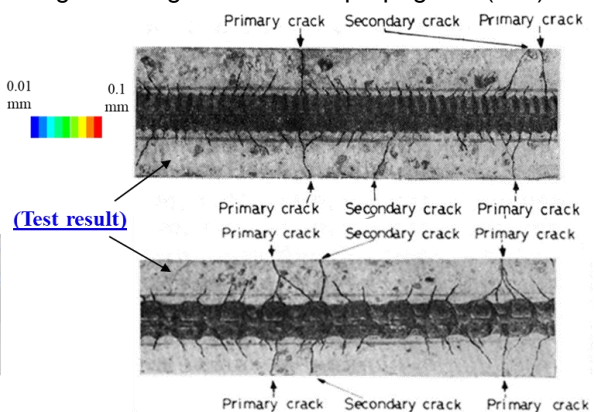
(Test result)

Fig. 18 Longitudinal crack propagation(x10)



(Lug spacing 30 mm)

Fig. 19 Effect of rebar lug spacing (Deformed Behavior x10, 3D and internal crack pattern)



(Test result)

cracks when rebar stress has become fairly high are called as secondary cracks. The crack patterns are only presented close to final stress stage of rebar investigated in test due to limited space available. The Fig. 17 shows the failure patterns at 305 MPa of rebar stress. In test, the inclination of the internal cracks was within 45 to 80

degrees to the bar axis and many of them were roughly 60 degrees and the maximum crack spacing was around 25 cm. In numerical simulation, the crack angle ranges between 60 to 80 degrees and most of cracks incline around 65 degrees and maximum crack spacing is approximately 26 cm. The Fig. 17 shows the propagation

of 3 secondary cracks to the surface of the prism in test at rebar stress of 300 MPa and numerical simulation also captures the 3 secondary cracks and their propagation to surface of prism at rebar stress of 305 MPa. The coupled RBSM-FEM model effectively captured the internal failure pattern of the axially loaded test specimens same as observed in the test. The Fig. 17 also confirms the formation of primary and secondary cracks around the deformed rebar, these numerical observations are consistent with test investigations. The Fig. 17 shows that the formation of internal cracks in concrete resembles comb like pattern as investigated in test, the deformation of concrete like comb shape causes the tightening of the concrete between the teeth of the comb as the steel tension is increased. The reaction of tightening force produces ring tension crack in concrete around the rebar. The formation of longitudinal cracks principally occurs because of ring tension. The formation of longitudinal cracks has been confirmed in numerical simulation as shown in Fig. 18 at 329 MPa rebar stress.

After verification for internal and longitudinal crack formation, the sensitivity of rebar lug spacing is also investigated. The numerical simulation results in this regard are shown in Fig. 19 around 300 MPa of rebar stress. The internal and 3D crack pattern clearly highlight the effect of rebar lug spacing on internal failure behavior although both specimens yield the splitting failure mode for same level of rebar stress. The internal crack pattern diagrams in Fig. 19 show that the specimen embedded with lug spacing of 30 mm produces more internal crack propagation and have more crack width in surrounding concrete compared with lug spacing of 15 mm. The coupled RBSM-FEM model, effectively captures the initiation and propagation of cracks and effect of rebar lug spacing.

The current research primarily focuses on the introduction and development of Voronoi mesh generation method for arbitrary shapes. Moreover, the validity of the proposed meshing method is confirmed using coupled RBSM-FEM model without highlighting the originality of the coupled RBSM-FEM model here, which is a subject of future research.

5. CONCLUSIONS

In this study, method to automatically generate arbitrary shapes such as deformed rebar considering geometrical details (core diameter, rib height, shape and lug spacing, etc.) is developed, using Voronoi mesh generation method and the validity of proposed method is also investigated.

- (1) The Voronoi mesh generation method is developed in order to overcome the limitation of meshing for complex shapes such as deformed rebar with rib shape, headed rebars and shear studs etc. in RBSM.
- (2) The proposed method has capability for automatic generation of Voronoi meshes that can represent the arbitrary shapes.
- (3) The reproducibility and usefulness of the proposed Voronoi mesh generation method has been confirmed through its application to meso-scale

simulation analysis for reinforced concrete (RC) prisms loaded in axial tensile force for failure patterns and bond behavior.

- (4) The numerical simulation results are found to be in good agreement with the experimental investigations. The numerical simulation results reveal the effectiveness and reliability of the proposed meshing method as numerically captured deformed behaviors and bond strength are observed to be consistent with the test results.

REFERENCES

- [1] Yamamoto, Y., Nakamura, H., Kuroda, I., and, Furuya, N., "Analysis of Compression Failure of Concrete by Three-Dimension Rigid Body Spring Model," *Doboku Gakkai Ronbunshuu*, Vol. 64(4), pp. 612-630, 2008. [in Japanese].
- [2] Yamamoto, Y., Nakamura, H., Kuroda, I., and, Furuya, N., "Crack Propagation Analysis of Reinforced Concrete Wall Under Cyclic Loading Using RBSM," *European Journal of Environmental and Civil Engineering*, Vol. 18, pp. 780-792, 2014.
- [3] Gedik, Y. H., Nakamura, H., Yamamoto, Y., and Kunieda, M., "Evaluation of Three-Dimensional Effects in Short Deep Beams using a Rigid-Body-Spring-Model," *Cement and Concrete Composites*, Vol. 33, pp. 978-991, 2011.
- [4] Hayashi, D., Nagai, K., and, Eddy, L., "Mesoscale Analysis of RC Anchorage Performance in Multidirectional Reinforcement using a Three-Dimensional Discrete Model," *J. Struct. Eng.*, Vol. 143, pp. 1-13, 2017.
- [5] Eddy, L., and Nagai, K., "Numerical simulation of Beam-Column Knee Joints with Mechanical Anchorage by 3D Rigid Body Spring Model," *Engineering Structures*, Vol. 126, pp. 547-558, 2016.
- [6] Cusatis, G., and Nakamura, H., "Discrete Modeling of Concrete Materials and Structures", *Cement and Concrete Composites* Vol. 33, pp.865-866, 2011.
- [7] Yamamoto, Y., "Evaluation of Failure Behaviors under Static and Dynamic Loadings of Concrete Members with Mesoscopic Scale Modeling," *Doctoral dissertation, Department of Civil Engineering, Nagoya University*, 2008.
- [8] Bolander Jr, J.E., Hong, G.S., and Yoshitake, K., "Structural Concrete Analysis using Rigid-Body-Spring Networks," *Computer-Aided Civil and Infrastructure Engineering*, Vol. 15, pp. 120-133, 2000.
- [9] Ikuma, K., Yamamoto, Y., Nakamura, H., and Miura, T., "Mesoscale Simulation of Bond Behavior of Deformed Rebar based on coupled RBSM-FEM method", *Proceedings of JCI annual convention* Vol. 40, pp.541-546, 2018. [in Japanese].
- [10] Sugihara, K., "Computational Geometry," *Baifukan.*, 1994, pp. 15-20. [in Japanese].
- [11] Goto, Y., "Cracks Formed in Concrete around Deformed Tension Bars," *ACI Journal*, Vol. 68, pp. 244-251, 1965.
- [12] Goto, Y., and Otsuka, K., "Experimental Studies on Cracks Formed in Concrete around Deformed Tension Bars," *J. JSCE*, Vol. 62, pp. 85-100, 1980. [in Japanese].